Since January 2020 Elsevier has created a COVID-19 resource centre with free information in English and Mandarin on the novel coronavirus COVID-19. The COVID-19 resource centre is hosted on Elsevier Connect, the company's public news and information website.

INSTITUT PASTEUR

Microbes and Infection 9 (2007) 96–102

www.elsevier.com/locate/micinf

Original article

Lipid rafts play an important role in the early stage of severe acute respiratory syndrome-coronavirus life cycle

Gui-Mei Li [a,1], Yong-Gang Li [a,b,1], Masanobu Yamate [a], Shu-Ming Li [a], Kazuyoshi Ikuta [a,b,*]

[a] *Department of Virology, Research Institute for Microbial Diseases (RIMD), Osaka University, Suita, Osaka 565-0871, Japan*
[b] *Research Collaboration Center on Emerging and Re-emerging Infections (RCC-ERI) of National Institute of Health-Department of Medical Sciences and RIMD-Osaka University, Nonthaburi 11000, Thailand*

Received 22 July 2006; accepted 23 October 2006
Available online 8 December 2006

Abstract

Lipid rafts are involved in the life cycle of many viruses. In this study, we showed that lipid rafts also play an important role in the life cycle of severe acute respiratory syndrome (SARS)-coronavirus (CoV). Cholesterol depletion by pretreatment of Vero E6 cells with methyl-β-cyclodextrin (MβCD) inhibited the production of SARS-CoV particles released from the infected cells. This inhibition was prevented by addition of cholesterol to the culture medium, indicating that the reduction of virus particle release was caused by the loss of cholesterol in the cell membrane. In contrast, cholesterol depletion at the post-entry stage (3 h post-infection) caused only a limited effect on virus particle release. Northern blot analysis revealed that the levels of viral mRNAs were significantly affected by pretreatment with MβCD, but not by treatment at 3 h post-infection. Interestingly, no apparent evidence for colocalization of angiotensin converting enzyme 2 with lipid rafts in the membrane of Vero E6 cells was obtained. These results suggest that lipid rafts could contribute to SARS-CoV infection in the early replication process in Vero E6 cells.

Keywords: Severe acute respiratory syndrome (SARS); Corona virus; Lipid rafts; Vero E6; ACE2

1. Introduction

Lipid rafts are special microdomains of the cell membrane where sphingolipids, cholesterol and associated proteins are enriched. Many biological events such as biosynthetic traffic, apoptosis, and signal transduction pathways require the integrity of rafts microdomains [1]. These membrane structures can be isolated on the basis of their insolubility in detergents such as Triton X-100 at 4 °C.

Accumulating evidence suggests that many pathogens, especially viruses, require lipid rafts at multiple stages of their life cycles. Human immunodeficiency virus type-1 (HIV-1), Semliki Forest virus and some human enteroviruses require lipid rafts during the binding and internalization of virus particles into host cells [2–4]. Interestingly, the receptors or co-receptors for certain viruses have been reported to be associated with lipid rafts on cell membranes, such as CD4 for HIV-1 [5], heat shock proteins 70 and 90 for dengue virus [6] and integrin αvβ3 for human cytomegalovirus [7]. Raft microenvironments also provide a platform for virus assembly as well as viral release. In the case of influenza virus, for example, both the cytoplasmic tail and the transmembrane domain of one of the viral proteins, hemagglutinin, facilitate the

Abbreviations: SARS, severe acute respiratory syndrome; CoV, coronavirus; MβCD, methyl-β-cyclodextrin; ACE2, angiotensin converting enzyme 2; HIV-1, human immunodeficiency virus type-1; MHV, murine hepatitis virus; TCID, tissue culture infectious dose; PBS, phosphate-buffered saline; MAb, monoclonal antibody; GAPDH, glyceraldehyde-3-phosphate dehydrogenase; TfR, transferrin receptor; PBST, PBS containing 0.1% Tween-20.

* Corresponding author. Department of Virology, Research Institute for Microbial Diseases (RIMD), Osaka University, 3-1 Yamadaoka, Suita, Osaka 565-0871, Japan. Tel.: +81 6 6879 8307; fax: +81 6 6879 8310.
E-mail address: ikuta@biken.osaka-u.ac.jp (K. Ikuta).

[1] G.M. Li and Y.G. Li contributed equally to this work.

1286-4579/$ - see front matter © 2006 Elsevier Masson SAS. All rights reserved.
doi:10.1016/j.micinf.2006.10.015

binding of another viral protein, matrix 1, to detergent-resistant lipid rafts [8]. Similarly, lipid rafts were also shown to be necessary for the assembly of HIV-1 [9] and Sendai virus [10]. Several enveloped viruses contain lipid rafts on their membranes, and cholesterol depletion by MβCD was shown to inactivate and permeabilize the virions, suggesting the importance of virus-associated cholesterol for infectivity [11,12]. Furthermore, Nef protein of HIV-1 is reported to be able to increase the infectivity of HIV-1 via lipid rafts [13]. Therefore, lipid rafts could play important roles not only in virus replication but also in viral pathogenesis.

Recently, the requirement for lipid rafts in the replication of coronaviruses (CoV), such as murine hepatitis virus (MHV), has been reported [14,15]. The cholesterol level on cell membranes determines their susceptibility to MHV infection. Further experiments revealed that MHV required lipid rafts for virus entry and fusion, but not for virus release [16]. The MHV receptor, carcinoembryonic antigen-related cell adhesion molecule 1, so-called CEACAM1, was shown not to be present in lipid rafts [15,16].

Severe acute respiratory syndrome (SARS)-CoV is a newly emergent member in the family *Coronaviridae* that cause a severe infectious respiratory disease [17,18]. Angiotensin converting enzyme 2 (ACE2) was found to be the receptor of SARS-CoV [19]. SARS-CoV can replicate well in Vero E6 cells and produce a large amount of progeny particles [20,21]. Although a recent report showed that SARS-CoV envelope protein was partially localized on lipid rafts and its transmembrane domain was required for maintenance of the membrane permeabilizing activity [22], there has been no direct evidence demonstrating the significance of lipid rafts during the replication of SARS-CoV. In the present study, we examined the significance of lipid rafts for the replication of SARS-CoV in Vero E6 cells. The data obtained revealed that lipid rafts in the cell membrane were required in the early stage of the replication of SARS-CoV.

2. Materials and methods

2.1. Cells and virus

The Vero E6 cell line was used for propagation of SARS-CoV (Frankfurt-1 strain) [23]. Vero E6 cells were maintained in MEM (Gibco BRL) supplemented with 10% fetal bovine serum (FBS; ICN Flow), 100 U/ml penicillin and 100 μg/ml streptomycin (GIBCO BRL) (complete medium) and passaged every 3 days. The inoculum of SARS-CoV was the culture medium from infected Vero E6 cells collected at 2 days post-infection. The virus titers were determined in 96-well microplates with Vero E6 cells and the result was expressed as 50% tissue culture infectious dose $(TCID)_{50}$/ml using Karber's method [24].

2.2. Assays for cholesterol level and cell viability

The Vero E6 cells seeded in 12-well microplates were left untreated or were pretreated with 10 mM MβCD (Sigma) for 30 min at 37 °C, as described previously [15]. After washing three times with phosphate-buffered saline (PBS), the cells were cultured in complete medium. After incubation for appropriate times post-treatment, cells were harvested and the lysate was assayed for cholesterol concentration using the Amplex Red Cholesterol Assay system (Molecular Probes). For cell viability assay, Vero E6 cells seeded in 96-well microplates were left untreated or were pretreated with MβCD similarly as described above. After incubation for appropriate times post-treatment, cells were subjected to viability assay by using a cell proliferation assay kit (Chemicon International) which examines the number of viable cells by measurement of the overall activity of the mitochondrial dehydrogenases in the sample. The formazan dye produced by viable cells can be quantified by measuring the absorbance of the dye solution at 450 nm.

2.3. Cholesterol depletion, replenishment and infection with SARS-CoV

The cells seeded in 6-well microplates were either left untreated or were treated with variable concentrations of MβCD for 30 min at 37 °C before incubation for 1 h with SARS-CoV at a multiplicity of infection (MOI) of 10, 0.1 or 0.001. Alternatively, cells were first incubated with SARS-CoV for 1 h, and then treated with 10 mM MβCD at 3 h after the adsorption. For each infection, cells were washed three times with PBS before culturing in MEM supplemented with 2% FBS. For cholesterol replenishment, cells were first pretreated with 10 mM MβCD for 30 min as described above, followed by supplementation of 400 μg/ml of cholesterol (Sigma) in MEM for 1 h at 37 °C. After three washes with PBS, the cells were subjected to mock-infection or infection with SARS-CoV. For investigation of the virus yield, cells were incubated for 18 h, and the culture supernatant was subjected to virus titration in Vero E6 cells, as described above.

2.4. Immunofluorescence assay

For analyses of viral antigen expression, immunofluorescence assay was performed as described previously [20]. Briefly, Vero E6 cells in an 8-well chamber that was left untreated or was treated with MβCD before infection or 3 h after infection. At 6 h post-infection (hpi), the cells were harvested and washed with PBS, and then fixed with 8% paraformaldehyde for 30 min at room temperature. The fixed cells were reacted with 3A2, a monoclonal antibody (MAb) against anti-SARS-CoV spike (S) protein [20].

2.5. Northern blot analysis

Northern blot analysis for SARS-CoV mRNAs was carried out as described previously, with some modifications [25]. Briefly, uninfected and infected Vero E6 cells either untreated or treated with MβCD were harvested. Total RNAs were extracted with Trizol (Invitrogen). RNAs (5 μg) were subjected to 1% agarose gel in the presence of formaldehyde, and blotted

onto a Hybond-N+ membrane (Amersham). A plasmid encoding the full-length nucleocapsid protein (N) gene, named pEFBOS-SARS-N, was constructed by introducing the full-length N gene into the pEFBOS vector. One fragment (28754–28323) of the gene was prepared as a probe by restriction enzyme digestion of the pEFBOS-SARS-N plasmid using *Nhe*I and *Xho*I [25]. The DNA probe (100 ng) was denatured at 100 °C for 5 min and then labeled with alkaline phosphatase using AlkPhos Direct™ Labeling and Detection Systems (GE Healthcare, Life Sciences). Blots were pre-hybridized with hybridization buffer at 55 °C for 1 h, and then subjected to hybridization with 10 ng/ml of alkaline phosphatase-labeled DNA probe at 55 °C for 18 h. After extensive washing, blots were developed with the CDP-star chemifluorescent detection system (AlkPhos Direct™ Labeling and Detection Systems). As a control for RNA input, a probe for glyceraldehyde-3-phosphate dehydrogenase (GAPDH) was also prepared by reverse transcriptase-PCR using SuperScript III Reverse Transcriptase (Invitrogen) with the RNAs isolated from uninfected Vero E6 cells. The primers for amplification were as follows: 5′-ACC ACA GTC CAT GCC ATC AC-3′ and 5′-TCC ACC ACC CTG TTG CTG TA-3′. The PCR products (100 ng) were labeled with alkaline phosphatase and used for hybridization with GAPDH mRNAs by procedures similar to those described above.

2.6. Flow cytometry analysis

To investigate whether cholesterol depletion affects the expression of ACE2 on the surface of Vero E6 cells, the cells were either left untreated or were pretreated with variable concentrations of MβCD at 37 °C for 30 min. After washing with PBS, the cells were detached by treatment with 10 mM EDTA. The detached cells were reacted with anti-human ACE2 MAb (R&D Systems). After reaction with fluorescent isothiocyanate conjugated goat anti-mouse IgG, the cells were subjected to flow cytometry analysis.

2.7. Membrane flotation assay

Vero E6 cells before and after adsorption with SARS-CoV at an MOI of 10 for 1 h at 37 °C were subjected to the membrane flotation assay according to a previously described procedure, with minor modifications [15]. Briefly, about 10^7 cells were washed three times in ice-cold PBS, and subsequently lysed in 1.0 ml of TNE buffer (50 mM Tris–HCl, pH 7.4, 100 mM NaCl, 1 mM EDTA) containing 1% Triton X-100. The lysate was homogenized by passage through a 27-gauge needle on a 1-ml syringe 20 times and subsequently centrifuged at 2000 rpm for 5 min at 4 °C to remove the cell nuclei and debris. The post-nuclear supernatant was incubated at 4 °C for 1 h and then mixed with 1 ml of ice-cold 80% (w/v) sucrose in TNE buffer. This mixture was put at the bottom of a Beckman SW50.1 ultracentrifuge tube, and overlaid with 2 ml of ice-cold 30% (w/v) sucrose in TNE buffer, and 1 ml of ice-cold 5% (w/v) sucrose in TNE buffer. Then, the sample was centrifuged at 35,000 × *g* at 4 °C for 17 h. Finally, 12 fractions were prepared from the top to the bottom of the tube and examined for the presence of ACE2 by Western blot analysis, as described below.

2.8. Western blot analysis

For Western blot analysis, each fraction obtained by membrane flotation assay was mixed at a 3:1 (v/v) ratio with 4× concentrated nonreducing sodium dodecyl sulfate–polyacrylamide gel electrophoresis sample buffer. Each fraction (20 μl) was subjected to sodium dodecyl sulfate–polyacrylamide gel electrophoresis. The Western blots were incubated with anti-human ACE2 MAb (R&D Systems), anti-human transferrin receptor (TfR) MAb (Zymed Laboratories, Invitrogen) or anti-caveolin-1 polyclonal antibody (Chemicon International) at 37 °C for 2 h. The blots were then washed three times in PBS containing 0.1% Tween-20 (PBST), and incubated with horseradish peroxidase-conjugated goat anti-mouse or anti-rabbit IgG (Jackson ImmunoResearch Laboratories) for 1 h at room temperature. Finally, the protein bands were visualized using the ECL plus Protein Detection System (Amersham).

2.9. Dot-blot analysis

For dot-blot analysis, a PVDF membrane (Immobilon-P, Millipore) was pretreated with methanol, followed by soaking in PBST for 5 min. Ten microliters of each sample fraction was dot-blotted on the membrane. After air-drying, the membrane was blocked with 1% bovine serum albumin in PBST at room temperature for 2 h. Ganglioside GM1 was detected with cholera toxin-peroxidase (Sigma) at 0.5 μg/ml for 30 min at room temperature, followed by washing 3 times with PBST, then the membrane was developed with the ECL plus Protein Detection System as described above.

3. Results

3.1. Depletion of cholesterol from the Vero E6 cell membrane by MβCD with no effect on the cell viability

To investigate the kinetics of the change of cholesterol level in Vero E6 cells, the cells were either left untreated or treated with 10 mM MβCD. These cells were collected just after treatment or 1, 3, 5, 7, and 9 h post-treatment. Cell lysates were prepared and subjected to the Amplex Red Cholesterol Assay. As shown in Fig. 1A, the cholesterol level decreased about 40% soon after the treatment. Subsequently, the level increased gradually to reach to the normal level at 5–7 h post-treatment. Thus, treatment of Vero E6 cells with 10 mM MβCD was able to remove cholesterol from the cells, as described in other reports [15].

To exclude the possibility that this concentration of MβCD might cause cell toxicity to Vero E6 cells, cell proliferation assays were performed at 0, 3, 9, and 24 h post-treatment. As shown in Fig. 1B, there was no apparent difference in the cell numbers between treated and untreated Vero E6 cells,

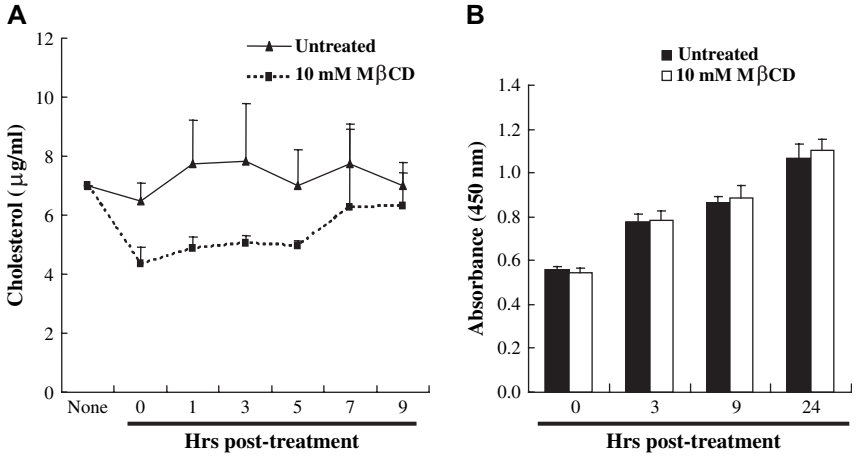

Fig. 1. Reduction of cholesterol levels in Vero E6 cells by MβCD treatment and its effect on cell proliferation. Semi-confluent monolayers of Vero E6 cells in 6-well microplates were left untreated or were treated with 10 mM MβCD. After washing three times with PBS, the cells were collected at the indicated time points and subjected to the Amplex Red Cholesterol Assay as well as the cell proliferation assay to show the effect of MβCD on cholesterol levels (A) and cell proliferation (B), respectively. Experiments were repeated three times and the arrow bars indicate the standard deviations of three independent experiments.

indicating no induction of cytotoxicity at a concentration of 10 mM MβCD.

3.2. Inhibition of SARS-CoV yield by MβCD treatment

Vero E6 cells were left untreated (Treat:N) or were pretreated with 5 mM and 10 mM MβCD for 30 min at 37 °C, then infected with SARS-CoV at various MOIs, i.e., 10, 0.1 and 0.001. These infected cells were cultured for 18 h. The virus production in the resulting culture fluid was assayed by titration on Vero E6 cells, as described in Section 2. The results were expressed as $TCID_{50}$ per ml. As shown in Fig. 2A, MβCD treatment impaired the virus production at a dose-dependent manner, suggesting that the cholesterol is necessary for the replication of SARS-CoV in Vero E6 cells. The impairment of the virus production was more apparent in cells infected with lower MOIs of SARS-CoV. To confirm the importance of cholesterol for SARS-CoV replication in Vero E6 cells, after depletion of cellular cholesterol by pretreatment with 10 mM MβCD for 30 min, cholesterol was added back (Treat:−0.5 + CHO) and then the virus production after replenishment was similarly investigated (Fig. 2B). The cholesterol replenishment could restore the virus production in all cases, as evidenced by similar levels of viral production as in untreated cells. These results suggest that the reduction of virus production was specifically due to the cholesterol depletion, and this effect was reversible. Next, we attempted to find out whether depletion of lipid rafts after the early stage of SARS-CoV life cycle has an inhibitory effect on virus production. Vero E6 cells were infected with SARS-CoV, and after incubation for 3 h, the cells were treated with MβCD (Treat:+3). At 18 hpi, virus production in the culture fluid was examined. As shown in Fig. 2B, the treatment after virus entry had only a mild effect, suggesting that cholesterol was

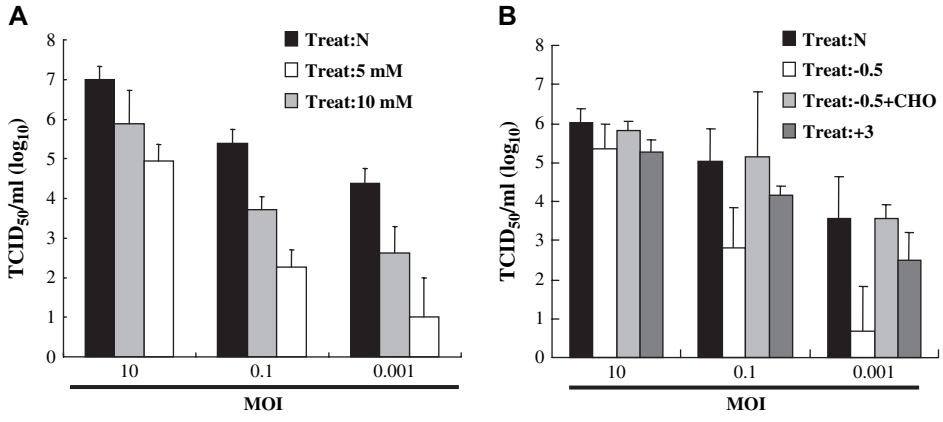

Fig. 2. Reduction of virus production by MβCD treatment. Vero E6 cells were left untreated (Treat:N) or were pretreated with 5 and 10 mM of MβCD for 30 min at 37 °C (Treat:-0.5), and then infected with SARS-CoV at an MOI of 10, 0.1, or 0.001. Alternatively, cells were first infected with SARS-CoV, as described above, and then treated with MβCD for 30 min at 37 °C at 3 hpi (Treat:+3). For cholesterol replenishment, the cells were first treated with MβCD for 30 min at 37 °C, followed by replenishment of cholesterol, and then cells were infected with SARS-CoV (Treat:−0.5 + CHO). After culturing for 18 h, the virus infectivity in the culture fluids was titrated in Vero E6 cells. Experiments were repeated three times and the arrow bars indicate the standard deviations of three independent experiments.

mainly required during the early stage of SARS-CoV replication.

3.3. Contribution of lipid rafts to the early stage of SARS-CoV replication

Next, the amounts of viral mRNAs inside the cells at 3 and 6 hpi were examined by Northern blot analysis. As shown in Fig. 3, at 3 hpi even at an MOI of 10, the level of viral mRNAs was significantly decreased in Vero E6 cells treated with MβCD at 30 min before infection (Treat:−0.5), compared with that in untreated cells (Treat: N), suggesting that virus entry was reduced by the depletion of cholesterol from the cell membrane. In addition, pretreated and untreated cells were similarly infected and at 3 hpi, cells were treated with MβCD (Treat:+3) and infected cells were incubated for another 3 h. When the viral mRNAs from the cells were compared, we found that at 6 hpi, cells pretreated with MβCD showed a significantly lower level of mRNA than untreated cells, but both types of cells showed much higher levels of viral mRNAs than at 3 hpi, indicating that mRNAs synthesis

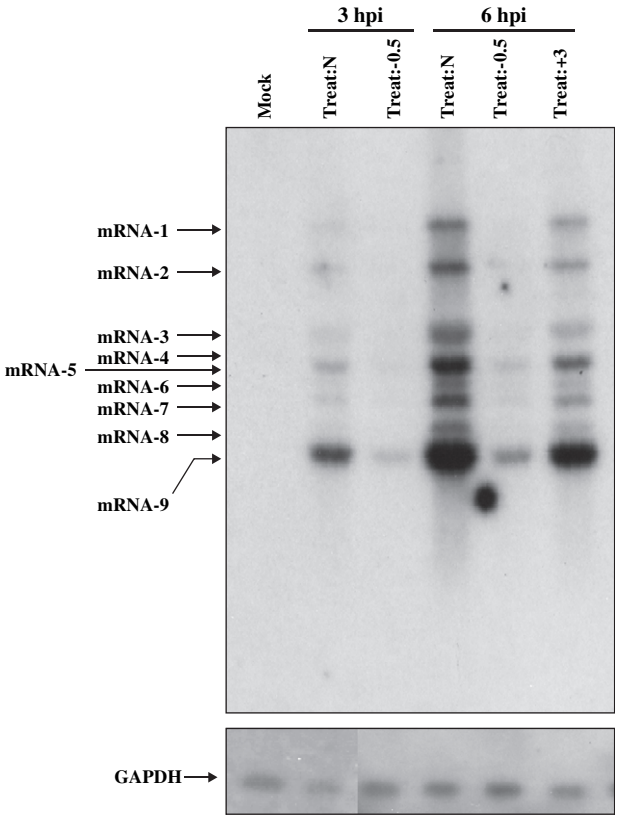

Fig. 3. Reduction of viral mRNA levels by MβCD treatment. Vero E6 cells were left untreated (Treat:N) or were pretreated with 10 mM MβCD for 30 min at 37 °C (Treat:−0.5), and then infected with SARS-CoV at an MOI of 10. Alternatively, cells were first infected with SARS-CoV, as described above, and then treated with MβCD for 30 min at 37 °C at 3 hpi (Treat:+3). After culturing for 3 and 6 h, respectively, total RNAs were extracted and subjected to Northern blot analysis with a DNA probe for the SARS-CoV N gene. As a control for RNA input, the same amounts of the RNA samples were subjected to Northern blot analysis for GAPDH gene expression.

was proceeded successfully. The treatment with MβCD at 3 hpi caused only a moderate effect, suggesting that the reduction of viral mRNA synthesis may have resulted from the blockage of an early process before starting the synthesis of viral messages. In addition, when immunofluorescence was performed to examine the viral antigen expression level using a MAb against SARS-CoV S protein, a clear reduction of viral antigen expression at 6 hpi was observed in the cells pretreated with 10 mM MβCD when infected at an MOI of 10 (data not shown).

3.4. No direct colocalization of ACE2 with lipid rafts

Flow cytometric analysis revealed that cholesterol extraction by MβCD treatment could reduce the expression level of cell surface ACE2 at a dose-dependent manner (Fig. 4A), suggesting that there may be some association of ACE2 with lipid rafts. We therefore performed membrane flotation assays to examine the localization of ACE2 in Vero E6 cells before or after SARS-CoV adsorption. As shown in Fig. 4B (upper four panels), ACE2 was mainly detected in fractions 9, 10 and 11, where TfR, used as a non-raft marker, was also enriched. Markers of lipid raft fractions, Caveolin-1 and GM1, were shown to be localized in the detergent-resistant membrane fractions, where ACE2 was not enriched. The data above suggested that ACE2 were not directly associated with lipid rafts. Next, we further examined possible shift of ACE2 location after virus adsorption (Fig. 4B, lower two panels). However, no apparent shift of ACE2 to rafts area was observed, suggesting that the virus binding could not trigger the re-localization of ACE2 in rafts membranes.

4. Discussion

Lipid rafts in the Vero E6 cell membrane were shown here for the first time to be necessary for the replication of SARS-CoV. Depletion of cholesterol by MβCD pretreatment significantly inhibited the virus production, especially when cells were infected at a low MOI. Subsequent experiments revealed that this inhibition probably was caused by blockage of early step of virus replication.

An investigation of virus infectivity revealed that cholesterol depletion impaired the virus production. The inhibitory effects could be reversed by replenishing cholesterol, implying the direct involvement of cholesterol in this process. The extent of the inhibition seemed to be dependent on the MOIs, although this finding might have resulted from the long incubation time that was needed for the virus infectivity assay. Since the cholesterol level in cell membranes was shown to be able to gradually increase to a similar level to that in untreated cells at 7–9 h post-treatment, the susceptibility of the cells to SARS-CoV infection might also have recovered, which would enable the next round of infection, especially when we infected the cells at higher MOI. This could be the reason for the less significant effects of MβCD pretreatment in the cells infected at higher MOIs, especially when we evaluated the effect of MβCD by virus infectivity.

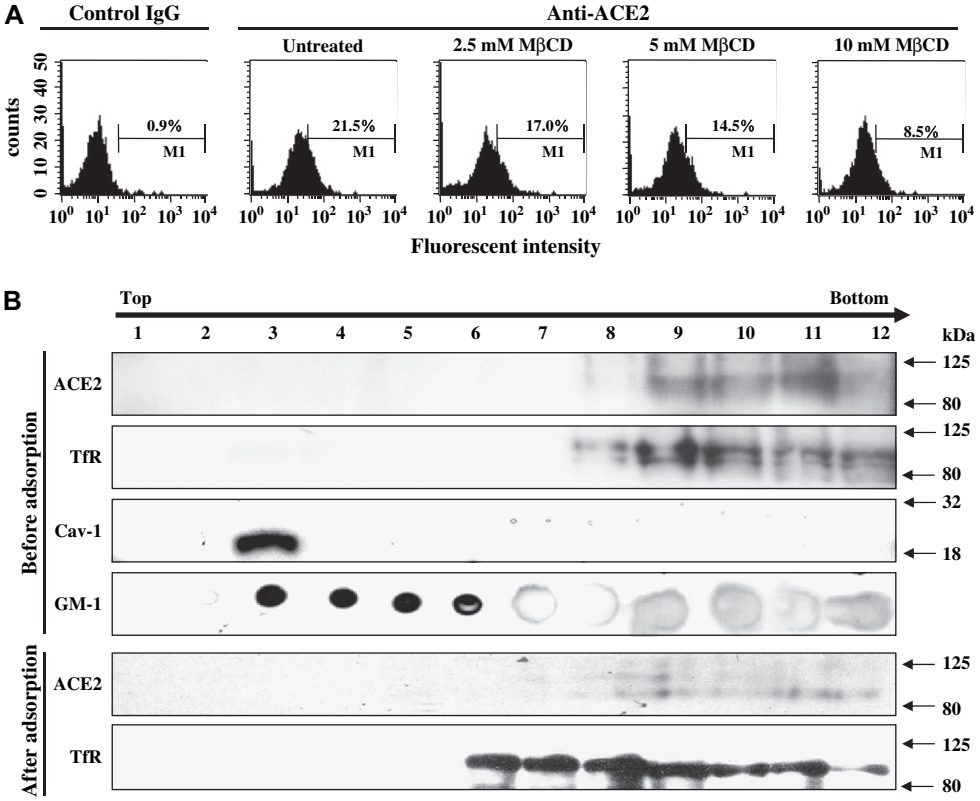

Fig. 4. No direct colocalization of ACE2 with lipid rafts. (A) Vero E6 cells were left untreated or were pretreated with 2.5, 5, and 10 mM MβCD for 30 min at 37 °C, and then the cells were subjected to flow cytometry analysis with antibody against ACE2. (B) Vero E6 cells before (upper four panels) or after adsorption with SARS-CoV at an MOI of 10 for 1 h at 37 °C (lower two panels) were subjected to the membrane flotation assay, as described in Section 2. After the ultracentrifugation, the samples in the tube were separated into 12 fractions. The fractions were Western-blotted and probed with antibodies against ACE2, TfR, and Cav-1. For detection of GM-1, the same fractions were dot-blotted and reacted with cholera toxin-peroxidase. Finally, these blots were visualized using the ECL Protein Detection System.

SARS-CoV was shown to be able to enter Vero E6 cells by fusion with cell membranes at 3 h after adsorption [26]. In this study, to investigate whether lipid rafts play a role in post entry step(s) or not, we treated the cells at 3 hpi. Both the results on virus particle release and virus antigen expression revealed that the Treat:+3 caused little inhibition of SARS-CoV replication, suggesting that cholesterol is mainly required in the early stages. Analysis of virus mRNA expression by Northern blotting suggested that the extent of virus entry was greatly reduced by depletion of cholesterol from the cell membrane, again indicating that cholesterol was required during the early stage of virus replication.

Many viruses utilize receptors that localize in raft microdomains of host cells for successful entry. We therefore examined the ACE2 expression level after MβCD treatment by flow cytometry. The result showed that MβCD treatment slightly decreased the expression level of ACE2 in the cell membrane at a dose-dependent manner. Thus, there might be some association between ACE2 and lipid rafts in the cell membrane. However, membrane flotation assays showed that ACE2 was not colocalized with lipid rafts in Vero E6 cells either uninfected or adsorbed with SARS-CoV. This result may be consistent with another report showing that ACE2 were not raft-colocalized in CHO cells [27]. In the case of HIV-1, major receptor CD4 is localized in lipid rafts, whereas the coreceptor CXCR4 is not directly associated with lipid rafts [5]. However, CXCR4 functionally requires cholesterol in target cells membranes [28]. Consequently, the discrepancy obtained by flow cytometry and membrane flotation assay in our study may be explained by the possible presence of unknown host factor(s) that could be localized in lipid rafts and play a role in the virus entry. SARS-CoV is known to utilize both endocytosis and fusion process to enter host cells [29]. Both pathways could be impaired by the extraction of cholesterol from cell membrane [1]. Further detail experiments would be necessary for determination which pathway was blocked by MβCD treatment.

Our results seem to be consistent with the findings obtained about MHV [15,16]. Lipid raft membrane structures were shown to be required for the entry, but not the viral particle release of MHV. The cellular receptor for MHV, CEACAM-1, was not enriched in raft-containing membranes. Cholesterol depletion had no effect on the binding of the virus to the cells; however, virus entry and virus-induced fusion were impaired, suggesting that cholesterol might be required at a post-binding stage [20]. In the case of another coronavirus, human coronavirus 229E (HCoV-229E), the cellular receptor CD13 was shown to be localized in the lipid rafts. The colocalization of HCoV-229E and caveolin-1 occurred under physical conditions; however, depletion of cholesterol by pretreatment with

MβCD reduced the colocalization without a significant effect on the binding of virus to cells. The depletion of cholesterol with MβCD significantly reduced the HCoV-229E redistribution and subsequent infection [30].

In the present study, we found that lipid rafts were required for the early stage of SARS-CoV replication and cholesterol may be required during the post-binding stage, as found for MHV [16]. Further detailed studies will be needed for understanding the mechanism to inhibit the SARS-CoV life cycle as well as for the possible application of this finding to the design for anti-SARS-CoV therapy.

Acknowledgments

We are grateful to Dr. John Ziebuhr, University of Würzburg, Germany for giving us the Frankfurt strain of SARS-CoV through Dr. Fumihiro Taguchi, National Institute of Infectious Diseases, Tokyo, Japan. This work was supported in part by a grant-in-aid for scientific research from the Ministry of Education, Science, Sports and Culture of Japan and the 21st Century COE program (Combined Program on Microbiology and Immunology) from the Japan Society for the Promotion of Science.

References

[1] N. Chazal, D. Gerlier, Virus entry, assembly, budding, and membrane rafts, Microbiol. Mol. Biol. Rev. 67 (2003) 226–237.
[2] S.L. Kozak, J.M. Heard, D. Kabat, Segregation of CD4 and CXCR4 into distinct lipid microdomains in T lymphocytes suggests a mechanism for membrane destabilization by human immunodeficiency virus, J. Virol. 76 (2002) 1802–1815.
[3] A. Ahn, D.L. Gibbons, M. Kielian, The fusion peptide of Semliki Forest virus associates with sterol-rich membrane domains, J. Virol. 76 (2002) 3267–3275.
[4] A.D. Stuart, H.E. Eustace, T.A. McKee, T.D. Brown, A novel cell entry pathway for a DAF-using human enterovirus is dependent on lipid rafts, J. Virol. 76 (2002) 9307–9322.
[5] W. Popik, T.M. Alce, W.C. Au, Human immunodeficiency virus type 1 uses lipid raft-colocalized CD4 and chemokine receptors for productive entry into CD4 $^{+}$ T cells, J. Virol. 76 (2002) 4709–4722.
[6] J. Reyes-Del Valle, S. Chavez-Salinas, F. Medina, R.M. Del Angel, Heat shock protein 90 and heat shock protein 70 are components of dengue virus receptor complex in human cells, J. Virol. 79 (2005) 4557–4567.
[7] X. Wang, D.Y. Huang, S.M. Huong, E.S. Huang, Integrin αβ3 is a coreceptor for human cytomegalovirus, Nat. Med. 11 (2005) 515–521.
[8] G.P. Leser, R.A. Lamb, Influenza virus assembly and budding in raft-derived microdomains: a quantitative analysis of the surface distribution of HA, NA and M2 proteins, Virology 342 (2005) 215–227.
[9] S. Manes, G. del Real, R.A. Lacalle, P. Lucas, C. Gomez-Mouton, S. Sanchez-Palomino, R. Delgado, J. Alcami, E. Mira, A.C. Martinez, Membrane raft microdomains mediate lateral assemblies required for HIV-1 infection, EMBO Rep. 1 (2000) 190–196.
[10] A. Ali, D.P. Nayak, Assembly of Sendai virus: M protein interacts with F and HN proteins and with the cytoplasmic tail and transmembrane domain of F protein, Virology 276 (2000) 289–303.
[11] Z. Liao, D.R. Graham, J.E. Hildreth, Lipid rafts and HIV pathogenesis: virion-associated cholesterol is required for fusion and infection of susceptible cells, AIDS Res. Hum. Retroviruses 19 (2003) 675–687.
[12] M. Takeda, G.P. Leser, C.J. Russell, R.A. Lamb, Influenza virus hemagglutinin concentrates in lipid raft microdomains for efficient viral fusion, Proc. Natl. Acad. Sci. USA 100 (2003) 14610–14617.
[13] Y.H. Zheng, A. Plemenitas, T. Linnemann, O.T. Fackler, B.M. Peterlin, Nef increases infectivity of HIV via lipid rafts, Curr. Biol. 11 (2001) 875–879.
[14] M. Daya, M. Cervin, R. Anderson, Cholesterol enhances mouse hepatitis virus-mediated cell fusion, Virology 163 (1988) 276–283.
[15] E.B. Thorp, T.M. Gallagher, Requirements for CEACAMs and cholesterol during murine coronavirus cell entry, J. Virol. 78 (2004) 2682–2692.
[16] K.S. Choi, H. Aizaki, M.M. Lai, Murine coronavirus requires lipid rafts for virus entry and cell-cell fusion but not for virus release, J. Virol. 79 (2005) 9862–9871.
[17] H. Osterhaus, H.W. SchmitzDoerr, Identification of a novel coronavirus in patients with severe acute respiratory syndrome, N. Engl. J. Med. 348 (2003) 1967–1976.
[18] K.V. Holmes, SARS-associated coronavirus, N. Engl. J. Med. 348 (2003) 1948–1951.
[19] W. Li, M.J. Moore, N. Vasilieva, J. Sui, S.K. Wong, M.A. Berne, M. Somasundaran, J.L. Sullivan, K. Luzuriaga, T.C. Greenough, H. Choe, M. Farzan, Angiotensin-converting enzyme 2 is a functional receptor for the SARS coronavirus, Nature 426 (2003) 450–454.
[20] M. Yamate, M. Yamashita, T. Goto, S. Tsuji, Y.G. Li, J. Warachit, M. Yunoki, K. Ikuta, Establishment of Vero E6 cell clones persistently infected with severe acute respiratory syndrome coronavirus, Microbes Infect. 7 (2005) 1530–1540.
[21] M. Yamashita, M. Yamate, G.M. Li, K. Ikuta, Susceptibility of human and rat neural cell lines to infection by SARS-coronavirus, Biochem. Biophys. Res. Commun. 334 (2005) 79–85.
[22] Y. Liao, Q. Yuan, J. Torres, J.P. Tam, D.X. Liu, Biochemical and functional characterization of the membrane association and membrane permeabilizing activity of the severe acute respiratory syndrome coronavirus envelope protein, Virology 349 (2006) 264–275.
[23] K.A. Ivanov, V. Thiel, J.C. Dobbe, Y. van der Meer, E.J. Snijder, J. Ziebuhr, Multiple enzymatic activities associated with severe acute respiratory syndrome coronavirus helicase, J. Virol. 78 (2004) 5619–5632.
[24] J. Karber, Beitrag zur kollectiven Behandlung pharmakologische Reihenversuche, Arch. Exp. Path. Pharmakol. 162 (1931) 480–483.
[25] V. Thiel, K.A. Ivanov, A. Putics, T. Hertzig, B. Schelle, S. Bayer, B. Weissbrich, E.J. Snijder, H. Rabenau, H.W. Doerr, A.E. Gorbalenya, J. Ziebuhr, Mechanisms and enzymes involved in SARS coronavirus genome expression, J. Gen. Virol. 84 (2003) 2305–2315.
[26] Q.F. Zhang, J.M. Cui, X.J. Huang, H.Y. Zheng, J.C. Huang, L. Fang, K.P. Li, J.Q. Zhang, The life cycle of SARS coronavirus in Vero E6 cells, J. Med. Virol. 73 (2004) 332–337.
[27] F.J. Warner, R.A. Lew, A.I. Smith, D.W. Lambert, N.M. Hooper, A.J. Turner, Angiotensin-converting enzyme 2 (ACE2), but not ACE, is preferentially localized to the apical surface of polarized kidney cells, J. Biol. Chem. 280 (2005) 39353–39362.
[28] D.H. Nguyen, D. Taub, CXCR4 function requires membrane cholesterol: implications for HIV infection, J. Immunol. 168 (2002) 4121–4412.
[29] Z.Y. Yang, Y. Huang, L. Ganesh, K. Leung, W.P. Kong, O. Schwartz, K. Subbarao, G. Nabel, pH-dependent entry of severe acute respiratory syndrome coronavirus is mediated by the spike glycoprotein and enhanced by dendritic cell transfer through DC-SIGN, J. Virol. 78 (2004) 5642–5650.
[30] R. Nomura, A. Kiyota, E. Suzaki, K. Kataoka, Y. Ohe, K. Miyamoto, T. Senda, T. Fujimoto, Human coronavirus 229E binds to CD13 in rafts and enters the cell through caveolae, J. Virol. 78 (2004) 8701–8708.